Supplementary Materials for

C1q restrains autoimmunity and viral infection by regulating CD8$^+$ T cell-metabolism

Guang Sheng Ling, Greg Crawford, Norzawani Buang, Istvan Bartok, Kunyuan Tian, Nicole M Thielens, Isabelle Bally, James A Harker, Philip G Ashton-Rickardt, Sophie Rutschmann, Jessica Strid, Marina Botto*

*Correspondence to: m.botto@imperial.ac.uk

This PDF file includes:

Materials and Methods
Figs. S1 to S15
References 27 to 38

Materials and Methods

Mice

C57BL/6 (B6) mice were purchased from Charles River Laboratories. Mice deficient in complement components C1q or C3 (*C1qa*$^{-/-}$ and *C3*$^{-/-}$ respectively) have previously been described (*27, 28*) and were backcrossed onto the B6 genetic background for 10 generations. B6.CD45.1^{+}, B6(C)-*H2-Ab1*^{bm12}/KhEgJ (bm12) (*29*) and OVA-specific TCR transgenic (C57BL/6-Tg(TcraTcrb)1100Mjb/J) (OT-I) (*30*) × *Rag1*$^{-/-}$ mice were purchased from Jackson Laboratories (Bar Harbor, USA). Female mice of 8-12 weeks of age were used. Control mice were age-, sex- and strain-matched. The animals were selected randomly from a large pool, but no specific method of randomization was used to allocate mice into groups. The number of animals for each experiment was determined based on previous experience with the models. No statistical methods were used to predetermine sample size. The investigators were not blinded to allocation during experiment and outcome assessment. Animals were kept in specific pathogen-free conditions and handled in accordance with institutional guidelines. All procedures were approved by the Imperial College AWERB committee and by the UK Home Office. The studies were conducted according to the ARRIVE guidelines.

Chronic graft-versus-host-disease (cGvHD)

cGvHD was induced by injecting i.p. complement-deficient mice and WT B6 mice with splenocytes (1×10^8) or magnetically purified CD4^{+} T cells (2×10^7) from age and sex-matched bm12 mice (*31*). Mice were bled at regular intervals as indicated. For CD8^{+} T-cell depletion, 200 μg of anti-CD8α Ab (clone YTS 169.4, BioXCell) or 200 μg of isotype-matched rat IgG2b

(Clone LFT-2, BioXCell) or PBS was administrated i.p. twice weekly throughout the duration of the experiment.

Lymphocytic choriomeningitis virus (LCMV) models

Mice were either infected i.p with 2×10^5 pfu of LCMV-Arm strain or i.v with 2×10^6 pfu of LCMV-Cl13 strain. In the recall response, mice were infected i.p. with 2×10^5 pfu of LCMV-Arm and 60 days later re-challenged i.v. with 10^6 pfu of LCMV-Cl13. Circulating LCMV viral titers were assessed using a quantitative PCR method as previously described (*32*). Virus-specific T cells were analyzed by flow cytometry using MHC-I dextramers (H-$2D^b$/np396-404, H-$2D^b$/gp33-41 and H-$2D^b$/gp276-286; Immundex). Splenocytes (10^6/well) from LCMV-infected mice were stimulated with MHC class I-restricted $NP_{396-404}$ (FQPQNGQFI), GP_{33-41} (KAVYNGATC), or $GP_{276-286}$ (SGVENPGGYCL) at 1 μg/ml (ProImmune) in the presence of brefeldin A and monesin (1×; all from eBioscience) for 5 hrs and stained for PE-conjugated anti-CD107a (clone 1D4B; 2 μg/ml; BD Pharmingen), PE-Cy7-conjugated anti-IFN-γ (clone XMG1.2; 2 μg/ml; ebioscience), FITC-conjugated anti-TNF-α (clone MP6-XT22; 10 μg/ml; BD Pharmingen) and APC-conjugated anti-IL-2 (clone JES6-5H4; 8 μg/ml; BD Pharmingen). The proportion of cytokine-producing cells within LCMV epitope-specific $CD8^+$ T cells was calculated as previously described (*33*). Lungs were taken from unperfused mice, fixed in 10% PBS buffered formalin, embedded in paraffin and stained with haematoxylin and eosin (H&E). The H&E stained sections were imaged using a 4 × objective and examined blindly. One lung section per mouse was scored for the presence of parenchymal edema. Scoring was as follows: edema present in 0 % of parenchyma = 0; 1% – 25% = 1; 25% – 50% = 2; 50% – 75% = 3; 75% – 100% = 4.

Autoantibody and renal assessment

MaxiSorp plates were coated with 100 /ml herring sperm DNA (Promega), 5 μg/ml chromatin (Arotec Diagnostic), 20 μg/ml RNP-SM (Arotec Diagnostic), 5 μg/ml Ro/SSA (Arotec Diagnostic), 5 μg/ml goat anti-mouse Ig H+L (SouthernBiotech) in borate-buffered saline. Serum samples were screened at 1:100 for autoantibody detection and at 1:200,000 for total IgG detection. Alkaline phosphatase–conjugated goat anti-mouse IgG (γ-chain specific; Sigma-Aldrich) was used as detection antibody (1:1,000 dilution). Autoantibody levels were expressed in arbitrary ELISA units relative to a standard positive sample derived from a serum pool from MRL/Mp-*Fas*^{lpr} mice. Serial dilutions of a known amount of IgG standard were used for total IgG detection. Kidneys were fixed in Bouin's solution and periodic acid–Schiff stained sections were blindly scored for glomerulonephritis (GN) as follows: grade 0 = normal; grade 1 = segmental hypercellularity in 10% – 25% of the glomeruli; grade 2 = hypercellularity involving >50% of the glomerular tuft in 25% – 50% of glomeruli; grade 3 = hypercellularity involving >50% of the glomerular tuft in 50% – 75% of glomeruli; grade 4 = glomerular hypercellularity in >75% or crescents in >25% of glomeruli. Quantitative glomerular immunostaining for C3 and IgG was performed on frozen sections using FITC-conjugated polyclonal goat anti-mouse C3 (2 μg/ml; MP Biomedicals) and FITC-conjugated polyclonal goat anti-mouse IgG Fc (1:200 dilution; Sigma-Aldrich) (*34*).

Lymphopenia-induced proliferation (LIP) and adoptive transfer experiments

B6.CD45.2^{+} recipients were given drinking water containing enrofloxacin (Baytril® 25 mg/ml) for 7 days before sub-lethal irradiation (600 rads) with a ^{137}Cs γ-ray source. One day later, naïve CD4^{+}CD44^{-}CD62L^{hi} or CD8^{+}CD44^{-}CD62L^{hi} T cells were magnetically purified (Miltenyi

Biotec) from B6.CD45.1^{+} mice, labelled with carboxyfluorescein succinimidyl ester (CFSE) at 5 μM and injected i.v. (10^6 cells/mouse) into antibiotic-treated sub-lethally irradiated B6.CD45.2^{+} recipients. At day 14 post-transfer, the proliferation and phenotype of the donor cells in the spleen were analyzed by flow cytometry.

Flow cytometry

Cells were treated with a saturating concentration of 2.4G2 monoclonal antibody (anti-CD16/32) to block Fc receptors and stained in PBS solution containing 1% BSA, 2mM EDTA, and 0.09% NaN_3. Isotype-matched control antibodies were used to determine the specificity of the staining. Fluorescence Minus One (FMO) controls were used to determine the gating boundaries. The following antibodies against mouse antigens were used: APC-conjugated anti-B220 (RA3-6B2; 1 μg/ml), BD Horizon™ BV711-conjugated anti-CD3ε (145-2C11; 2 μg/ml), PE-conjugated anti-CD11c (HL3; 2 μg/ml), PerCP-Cyanine5.5-conjugated anti-CD19 (1D3; 2 μg/ml), PE-conjugated anti-CD40 (3/23; 2 μg/ml), FITC-conjugated anti-CD62L (MEL-14; 10 μg/ml), PE-conjugated anti-CD62L (MEL-14; 2 μg/ml), PE-Cy7-conjugated anti-CD95 (Jo2; 2 μg/ml), PE-conjugated anti-CXCR5 (2G8; 2 μg/ml), Alexa Fluor®647-conjugated anti-Blimp-1 (5F7; 2 μg/ml), FITC-conjugated anti-TNF-α (clone MP6-XT22; 10 μg/ml), APC-conjugated anti-IL-2 (clone JES6-5H4; 8 μg/ml), PE-conjugated mouse IgG1 isotype control (MOPC-21; 5 μg/ml), all from BD Bioscience; APC-conjugated anti-CD4 (RM4-5; 2 μg/ml), APC-conjugated anti-CD11c (N418; 2 μg/ml), FITC-conjugated anti-CD44 (IM7; 2.5 μg/ml), APC-Cy7-conjugated anti-CD45 (30-F11; 1 μg/ml), APC-Cy7-conjugated anti-CD45.1 (A20; 1 μg/ml), PerCP-Cyanine5.5-conjugated anti-CD45.2 (104; 1 μg/ml), PE-Cy7-conjugated anti-CD127 (A7R34; 2 μg/ml), eFluor®450-conjugated anti-Eomes (Dan11mag; 2 μg/ml), eFluor®450-conjugated anti-GL7

(GL7; 2 μg/ml), PE-Cy7-conjugated anti-Granzyme B (NGZM; 2 μg/ml), FITC-conjugated anti-IA/IE (M5/114.15.2; 2.5 μg/ml), PE-Cy7-conjugated anti-IFN-γ (clone XMG1.2; 2 μg/ml), eFluor®450-conjugated anti-KLRG1 (2F1; 2 μg/ml), APC-conjugated anti-KLRG1 (2F1; 2 μg/ml), FITC-conjugated anti-KLRG1 (2F1; 5 μg/ml), PE-Cy7 conjugated anti-PD-1 (J43; 2 μg/ml), PE-conjugated anti-T-bet (eBio4B10(4B10); 2 μg/ml) and PE-conjugated rat IgG2a isotype control (eBR2a, 2 μg/ml), all from eBioscience; Alexa Fluor®488-conjugated anti-Bcl-2 (BCL/10C4, 5 μg/ml), Brilliant Violet 421™-conjugated anti-CD8α (53-6.7; 0.25 μg/ml), PerCP-Cyanine5.5-conjugated anti-CD8α (53-6.7; 2 μg/ml), Alexa Fluor®488-conjugated anti-CD11b (M1/70; 2.5 μg/ml), PerCP-Cyanine5.5-conjugated anti-CD44 (IM7; 1 μg/ml), FITC-conjugated anti-CD69 (H1.2F3; 5 μg/ml), APC-Cy7-conjugated anti-CD86 (GL-1; 2 μg/ml), PE-conjugated anti-CD127 (A7R34; 2 μg/ml) and FITC-conjugated rat IgG1 isotype control (RTK2071; 5 μg/ml) all from Biolegend. Antibodies against human antigens: PerCP-eFluor710-conjugated anti-CD25 (CD25-4E3; 1.2 μg/ml) and APC-conjugated anti-CD69 (FN50; 0.5 μg/ml) all from eBioscience; Brilliant Violet 421™-conjugated anti-CCR7 (G043H7, 14 μg/ml), APC-Cy7-conjugated anti-CD3ε (SK7; 13.3 μg/ml), APC-conjugated anti-CD8α (SK1; 1.66 μg/ml), Brilliant Violet 421™-conjugated anti-CD8α (SK1; 1.66 μg/ml), PE-conjugated anti-CD8α (SK1; 0.8 μg/ml), PerCP-Cyanine5.5-conjugated anti-CD45RA (HI100, 5 μg/ml), PE-conjugated anti-CD62L (DREG-56; 1.66 μg/ml), Brilliant Violet 785™-conjugated anti-CD127 (A019D5, 5 μg/ml), PE-conjugated anti-Granzyme B (QA16A02; 1 μg/ml), APC-conjugated anti-KLRG1 (14C2A07, 33 μg/ml), all from Biolegend. A polyclonal antibody against p32/gC1qR (40 μg/ml) and rabbit IgG isotype control (40 μg/ml) were purchased from Abcam. Spleen samples were dispersed and filtered through 70 μM cell strainer (Corning) to obtain

single-cell suspensions. To exclude dead cells from staining, Live/dead Fixable Aqua stain kit (Molecular Probes, Life Technologies) was used according to the manufacturer's instructions. OVA-specific $CD8^+$ T cells were detected using H-$2K^b$ SIINFEKL Pentamer (Proimmune); LCMV-specific $CD8^+$ T cells using MHC dextramers for LCMV gp33, np396 and gp276 epitopes (Immudex). Active Caspase 3/7 staining was carried out by incubating the cells with 500 nM CellEvent™ Caspase-3/7 Detection Reagent (Molecular Probes, Life Technologies) at 37 °C for 30 mins. For intracellular cytokine staining, cells were stimulated with PMA (25 ng/ml; Sigma-Aldrich) and ionomycin (1 μg/mL; Calbiochem) in the presence of GolgiSTOP (BD Bioscience) for 4 hrs at 37 °C. In some experiments cells were stimulated with LCMV peptides [FQPQNGQFI (np396), KAVYNGATC (gp33), or SGVENPGGYCL (gp276); 1 μg/ml; ProImmune] or OVA peptide (1 μM; InvivoGen). BD Cytofix/Cytoperm™ Plus Fixation/Permeabilization Kit (BD Bioscience) was then used according to the manufacturer's instructions. For intracellular Bcl-2, Blimp-1, T-bet and Eomes staining, the Foxp3 staining kit (eBioscience) was used as for manufacturer's instructions. Mitochondrial membrane potential was measured by incubating cells for 30 mins at 37 °C with 25 nM MitoTracker Deep Red FM (Molecular Probes, Life Technologies). Stained cells were acquired using a BD FACSVerse or a LSRFortessa Flow cytometer (BD Biosciences). Data were analyzed using FlowJo software, version 7.6.5 (TreeStar Inc, Ashland, OR, USA).

BrdU pulsing

Three doses of 2 mg of 5-bromo-2-deoxyuridine (BrdU) (Invitrogen) were administered i.p. for 3 consecutive days starting at day 11 after cGvH induction. BrdU incorporation in blood $CD8^+$ T cells was assessed by bleeding the mice 1, 3, and 6 days following the last BrdU injection. BrdU

incorporation was measured using the BrdU Staining Kit (eBioscience). BrdU decay rates were calculated as previously described (*35*).

Cell sorting and metabolic assays

Splenic $CD44^+CD62L^+CD8^+$ and $CD44^+CD62L^-CD8^+$ T cells were sorted at day 14 after cGvH induction using FACS Aria II (BD Biosciences). The metabolic profile of the sorted $CD8^+$ T cells (> 95% purity) was analyzed using XF Cell Mito Stress kit (Seahorse Bioscience). Briefly, cells were resuspended in serum-free unbuffered RPMI-1640 medium (R1383, Sigma-Aldrich) containing 2 mM L-glutamine, 1 mM sodium pyruvate, and 25 mM Glucose. Cells were seeded on 24-well polystyrene Seahorse plates pre-coated with Cell-Tak (Corning) at 7.5×10^5 cells/well. The culture was equilibrated for 1 hr at 37 °C and then assayed for the oxygen consumption rate (OCR) (pMole/min) and extracellular acidification rate (ECAR) (mpH/min) in response to 1 μM oligomycin, 1 μM fluorocarbonylcyanide phenylhydrazone (FCCP), 1 μM rotenone, and 1 μM antimycin A with the XF-24 Extracellular Flux Analyzer. OCR and ECAR measures were repeated three times of 3–2–3-min mix–wait–measure cycle. All samples were run in triplicate or quadruplicates.

In vitro experiments

OT-I T cells were labelled with 5 μM of Cell Proliferation Dye eFluor® 670 (eBioscience) and stimulated with 10^{-6} M OVA peptides: N4 (SIINFEKL), T4 (SIITFEKL), or G4 (SIIGFEKL) (Cambridge Bioscience) in RPMI-1640 medium (Invitrogen) supplemented with 10% FCS, 2 mM L-glutamine, 100 IU/ml penicillin, 100 μg/ml streptomycin, 50 μM 2-mercaptoethanol, and 10 mM HEPES. Cell proliferation was assessed by flow cytometry at 48 hrs in the presence or

absence of purified hC1q (80 μg/ml; Hycult). In some experiments, OT-I T cells were cultured for 24 hrs and then labelled with 0.5 μCi of [^{3}H] thymidine. Thymidine update was measured 16 hrs later.

Naïve OT-I CD8$^+$ T cells were purified with CD8a$^+$ T cell isolation kit (Miltenyi Biotec) and cultured (2 × 10^6 cells/well) in 12-well plates with SIINFEKL peptide (10^{-10}M) and IL-2 (20 ng/ml; PeproTech) for 3 days. Activated cells were then washed with PBS and cultured in 12-well plates at 5 × 10^5 cells/well with IL-2 (10 ng/ml; PeproTech) or in 6-well plates at 2.5 × 10^6 cells/well with IL-15 (50 ng/ml; PeproTech) (*36*) in the presence or absence of purified hC1q (80 μg/ml; Hycult) for another 4 days. Dead cells were eliminated with Dead Cell Removal Kit (Miltenyi Biotec) and RNA was extracted from alive cells using the RNeasy mini kit (Qiagen).

Splenic CD8$^+$ T cells were purified from naïve WT mice using the CD8a$^+$ T cell isolation kit (Miltenyi Biotec) and cultured (1 × 10^5 cells/well) for 48 hrs untreated or activated with anti-CD3/CD28 beads (Gibco; 1 × 10^5 beads/well) in the presence or absence of rapamycin (Calbiochem), an mTORC1 inhibitor (500 nM). For other metabolic conditions, CD8$^+$ T cells were first activated with anti-CD3/CD28 beads for 24 hrs and then cultured for another 24 hrs in the presence of 2-deoxyglucose (Sigma-Aldrich; 2DG) (50 mM) or glucose-free medium or galactose medium (10 mM), to prevent cells utilizing glycolysis (*37*), or oligomycin (Sigma-Aldrich; 10 nM) or fluorocarbonylcyanide phenylhydrazone (FCCP) (Sigma-Aldrich; 10 nM) or serum-free medium. p32/gC1qR surface expression was measured by flow cytometry.

Purified splenic CD8$^+$ T cells from *C1qa*$^{-/-}$ mice were stimulated with anti-CD3/CD28 beads (Gibco; 1 × 10^5 beads/well) for 24 hrs. Activated cells were left untreated or treated with Dynasore (Sigma-Aldrich; 100 μM) in serum-free medium for 1 hr. Cells were then incubated with hC1q (80 μg/ml; Hycult) for another 30 mins. After washing, cells were kept at 4 °C or 37

°C and surface expression of C1q was assessed by flow cytometry with FITC-conjugated anti-C1q antibody (JL-1; 1 μg/ml; Hycult) at three time points: 0, 30, and 60 mins. The surface loss of C1q was expressed as the fraction of $CD8^+$ T cells remaining C1q positive at 30 and 60 mins relative to the corresponding time 0.

Healthy volunteer blood samples were collected as a sub-collection registered with the Imperial College Healthcare Tissue Bank (NRES approval 12/WA/0196). Informed consent was obtained from all contributing individuals according to the Declaration of Helsinki. Peripheral blood mononuclear cells (PBMCs) were isolated using the Lymphoprep™ (STEMCELL technologies) gradient separation and labelled with 2.5 μM CFSE. Cells were plated at 10^5 cells/well and stimulated with Dynabeads®Human T-Activator CD3/CD28 beads (ranging from 0.07×10^5 to 2×10^5 beads/well; Gibco) or with concanavalin A (ranging 1 to 10 μg/ml; Sigma) in the presence or absence of 50 μg/ml of hC1q (Hycult) in a total volume of 200 μl. Cell activation was assessed by CD25 and CD69 expression level at 24 hrs and cell proliferation by CFSE dilution at 72 hrs by flow cytometry. Human $CD8^+$ T cells were purified using the Dynabeads® FlowComp™ Human CD8 cell isolation kit (Invitrogen). Cells were plated at 8×10^4 cells/well and stimulated with Dynabeads®Human T-Activator CD3/CD28 beads (ranging from 0.8×10^4 to 8×10^4 beads/well; Gibco) in the presence or absence of 50 μg/ml of hC1q (Hycult) in a total volume of 200 μl. Expression of KLRG1, IL-7R, CD45RA, CD62L and Granzyme B was assessed by flow cytometry. IFNγ secretion was measured by ELISA (R&D Systems) at 24 and 72 hrs.

Immunization with dead cells

OVA-expressing H-2^{bm1} mouse embryonic fibroblasts (OVA-MEFs) (*11*) were exposed to UV light (240 mJ/cm^2) and further cultured for 16 hrs in complete medium resulting in more than 85% of dead cells. WT or *C1qa*$^{-/-}$ mice received i.v. 10^6 CFSE-labelled OT-I cells. One day later, 10^5 UV-treated OVA-MEFs were injected i.v., OT-I proliferation in the spleen was analyzed at 48 and 72 hrs. CD44, CD62L, KLRG1, IL-7R, T-bet, and Eomes expression in splenic OT-I cells was assessed by flow cytometry at day 5. Intracellular cytokine production was measured following in vitro incubation with 1 μM OVA peptide for 4 hrs.

C1q binding

Blood cells from *C1qa*$^{-/-}$ mice were incubated with purified hC1q (80 μg/ml; Hycult), 30% normal mouse serum (NMS), or 30% *C1qa*$^{-/-}$ mouse serum in PBS 1% BSA for 30 mins at 37 °C. After wash, surface C1q was detected with FITC-conjugated anti-mouse C1q mAb (JL-1, 1 μg/ml; Hycult) by flow cytometry. The globular and collagen-tail fragments of hC1q were generated by limited collagenase and pepsin digestion and purified as described previously (*38*). In competition experiments, blood cells were pre-incubated with the globular or the collagen fragments (two doses: 25 μg/ml and 50 μg/ml) in PBS 1% BSA for 30 mins at 37 °C prior to the addition of purified hC1q (50 μg/ml).

Confocal imaging

IL-15-differentiated OT-I $CD8^+$ T cells, prepared as described above, were transferred into a 24-well plate with BioCoat poly-L-lysine slides (Corning). Cells were incubated with purified hC1q (100 μg/ml; Hycult) for 1 hr, followed by MitoTracker® Orange CMTMRos (100 nM; Molecular Probes, Life Technologies) for 30 mins at 37 °C. Cells were then washed with PBS,

fixed with 4% formaldehyde, and permeabilized with ice-cold methanol. After blocking with PBS, 5% normal goat serum, and 0.3% Triton, C1q was detected with FITC-conjugated anti-C1q antibody (Clone JL-1, 1 μg/ml; Hycult). p32/gC1qR was visualized with polyclonal anti-p32/gC1qR antibody (2.5 μg/ml; Abcam) and a goat anti-rabbit IgG-AF647 (2 μg/ml; Molecular Probes, Life Technologies) in PBS and 0.3% Triton. Coverslips were mounted in Vectashield with DAPI (Vector Laboratories). Confocal fluorescence images were acquired on a LSM780 scanning confocal microscope with a 63 × oil immersion DIC Plan-Apochromat objective and GaAsP detection system (Carl Zeiss). Images were processed and analyzed using Image J software (version 2.0.0; NIH).

Quantitative PCR (qPCR)

Total RNA was extracted using RNeasy mini kit (Qiagen). RNA was quantified by absorbance spectroscopy (Nanodrop) and converted to cDNA by reverse-transcriptase reaction (iScript cDNA synthesis kit; Bio-rad). qPCR analysis was performed on an Applied Biosystems 7500 real-time qPCR machine using SYBR gene amplification detection reagent (Applied Biosystems). Expression levels were compared using the ΔΔCt method normalized to 18S ribosomal and expressed as fold change relative the samples without C1q addition. Primer pairs used were: *Tfam* (forward, 5′-GCTCTACACGCCCCTGGTTTCTGG-3′; reverse, 5′-TCGCTGTAGTGCCTGCTGCTCCTG-3′), *Ppargc1a* (forward, 5′-CCCTGCCATTGTTAAGACC-3′; reverse, 5′-TGCTGCTGTTCCTGTTTTC-3′), *Ppargc1b* (forward, 5′-CTTGCTAACATCACAGAGGATATCTTG-3′; reverse, 5′-GGCAGGTTCAACCCCGA-3′), *Nrf1* (forward, 5′-TATGGCGGAAGTAATGAAAGACG-3′; reverse, 5′-CAACGTAAGCTCTGCCTTGTT-3′), *Ndufs8* (forward, 5′-

TGGCGGCAACGTACAAGTAT-3′; reverse, 5′- CCTCGGATGAGTTCTGTCCA-3′), *Shda* (forward, 5′-GAAAGGCGGGCAGGCTCATC-3′; reverse, 5′-CACCAGGCACTCCCCATTTT-3′), *Cox5a* (forward, 5′-TTGATGCCTGGGAATTGCGTAAAG-3′; reverse, 5′-AACAACCTCCAAGATGCGAACAG-3′), *Apt5l* (forward, 5′-GAGAAGGCACCGTCGATGG-3′; reverse, 5′-ACACTCTGAATAGCTGTAGGGAT-3′), *Cpt1a* (forward, 5′-CCAGGCTACAGTGGGACATT-3′; reverse, 5′-GAACTTGCCCATGTCCTTGT-3′), *Cpt2* (forward, 5′-GGCCAGGGCTTTGACCGACACT-3′; reverse, 5′-TGCCAAAGCCATCAGGGACCAC-3′), *Cd36* (forward, 5′-GATGTGGAACCCATAACTGGATTCAC-3′; reverse, 5′-GGTCCCAGTCTCATTTAGCCACAGTA-3′), *Scd1* (forward, 5′-AAAGAGAAGGGCGGAAAAC-3′; reverse, 5′-GCGTTGAGCACCAGAGTGTA-3′), *Acaca* (forward, 5′-CCCAGCAGAATAAAGCTACTTTGG-3′; reverse, 5′-TCCTTTTGTGCAACTAGGAACGT-3′), *Slc2a1* (forward, 5′-CAGTTCGGCTATAACACTGGTG-3′; reverse, 5′-GCCCCCGACAGAGAAGATG-3′), *Hk2* (forward, 5′-TGATCGCCTGCTTATTCACGG-3′; reverse, 5′-AACCGCCTAGAAATCTCCAGA-3′), *Pdk1* (forward, 5′-GGACTTCGGGTCAGTGAATGC-3′; reverse, 5′-TCCTGAGAAGATTGTCGGGGA-3′), *Pgm1* (forward, 5′-CAGAACCCTTTAACCTCTGAGTC-3′; reverse, 5′-CGAGAAATCCCTGCTCCCATAG-3′), *Pkm2* (forward, 5′-TGCCGTGCTGAATGCCTGGG-3′; reverse 5′-CGCCACCCGGTCAGCACAAT-3′), *18S* (forward, 5′-CCGCAGCTAGGAATAATGGAAT-3′; reverse 5′-CGAACCTCCGACTTTCGTTCT-3′), *Bcl-2* (forward, 5′-AGCCTGAGAGCAACCCAAT-3′; reverse, 5′-ATAGTTCCACAAAGGCATCCCAG-3′),

Prdm1 (forward, 5′-ATGGAGGACGCTGATATGAC-3′; reverse, 5′-CCTTACTTACCACGCCAATAAC-3′).

Statistical analysis

Data are expressed as mean ± SEM unless otherwise stated. Comparisons between two groups were analyzed using unpaired two-tailed Student's *t*-test. Multiple corrections were analyzed using one-way ANOVA with Bonferroni corrections or two-way ANOVA with the Tukey–Kramer test. Non-parametric data were analyzed by the Mann–Whitney test or Kruskal–Wallis test. In some experiments, a paired Student's *t*-test or Wilcoxon signed-rank test was applied as indicated. p values of <0.05 were considered statistically significant. Statistical analyses were performed with GraphPad Prism 7.0 (Graph Pad software).

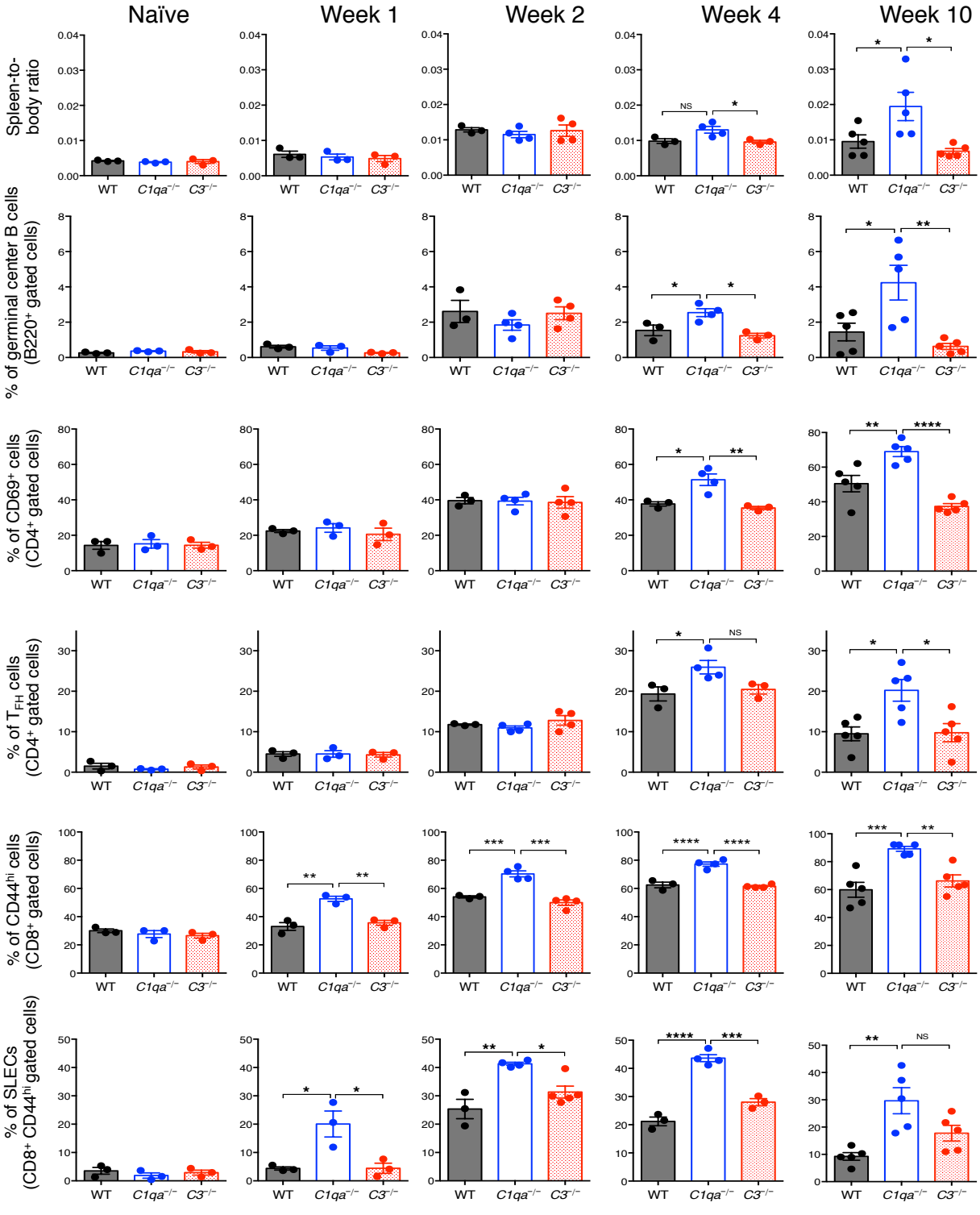

Fig. S1. Splenic bm12-cGvH response in WT, *C1qa*$^{-/-}$ and *C3*$^{-/-}$ mice. Spleen-to-body mass ratio, percentages of germinal center B cells (GL7^{+}Fas^{+}), T_{FH} (CXCR5^{+}PD-1^{+}), CD4^{+}CD69^{+}, CD8^{+}CD44^{hi}, and SLEC (KLRG1^{+}IL-7^{-}) cells were compared at one week (n = 3 mice/group), two weeks (n = 3-4 mice/group), four weeks (n = 3-4 mice/group), and ten weeks (n = 5 mice/group) after bm12 injection. Spleens from naïve mice were used as controls (n = 3 mice/group). NS: not significant; *p<0.05; **p<0.01; ***p<0.005; ****p<0.0001; one-way ANOVA. Data are mean ± SEM and represent two-to-three experiments.

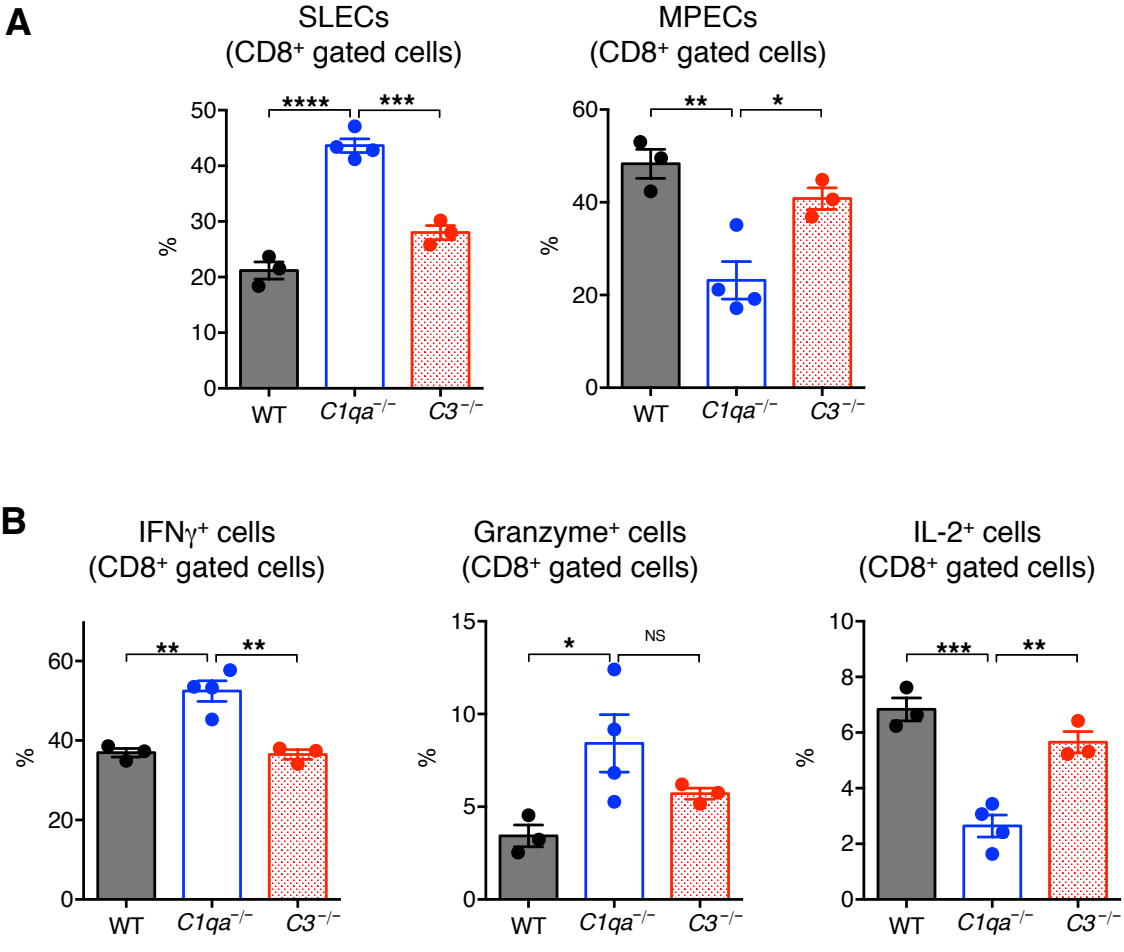

Fig. S2. CD8$^+$ T-cell response is skewed towards an effector phenotype in *C1qa*$^{-/-}$ but not in *C3*$^{-/-}$ mice after cGvH induction. (A) Splenocytes were isolated from bm12-cGvH recipients four weeks after disease induction. Proportions of SLECs (CD44^{hi}KLRG1$^+$IL-7R$^-$) and MPECs (CD44^{hi}KLRG1$^-$IL-7R$^+$) among the CD8$^+$ T cells determined by flow cytometry. **(B)** Fractions of splenic CD8$^+$ T cells expressing IFNγ, Granzyme B, or IL-2 after in vitro restimulation. NS: not significant; *p<0.05; **p<0.01; ***p<0.005; ****p<0.0001; one-way ANOVA. Data are mean ± SEM and represent three experiments (n = 3-4 mice/group).

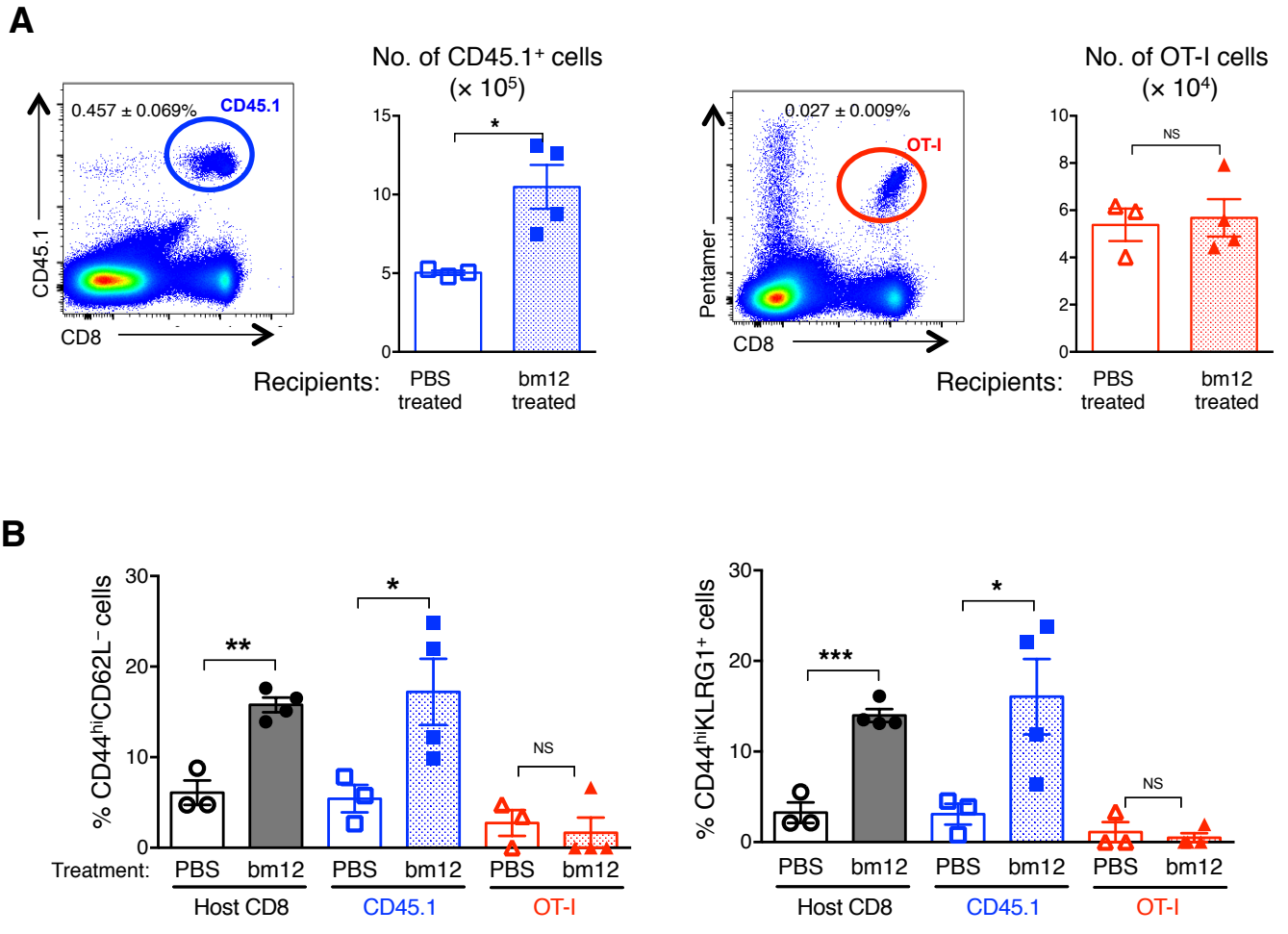

Fig. S3. In bm12-cGvHD model CD8$^+$ T-cell activation is driven by TCR-specific signals. (A) Naïve CD8$^+$ T cells from B6.CD45.1$^+$ and OT-I mice were mixed at 1:1 ratio and co-transferred into B6.CD45.2$^+$ mice. One day later the recipients were i.p injected with either PBS or bm12 splenocytes. Representative flow plots and absolute number of splenic CD8$^+$CD45.1$^+$ T cells (left) and pentamer$^+$OT-I cells (right) recovered ten days after GvH induction. **(B)** Percentages of CD44^{hi}CD62L$^-$ and CD44^{hi}KLRG1$^+$ cells: gated host CD8$^+$ (CD45.1$^-$pentamer$^-$), adoptively transferred CD8$^+$ (CD45.1$^+$) and OT-I (pentamer$^+$) T cells. NS: not significant; *p<0.05; **p<0.01; ***p<0.001; unpaired Student's t-test. Data are mean ± SEM and represent three experiments (n = 3-4 mice/ group)

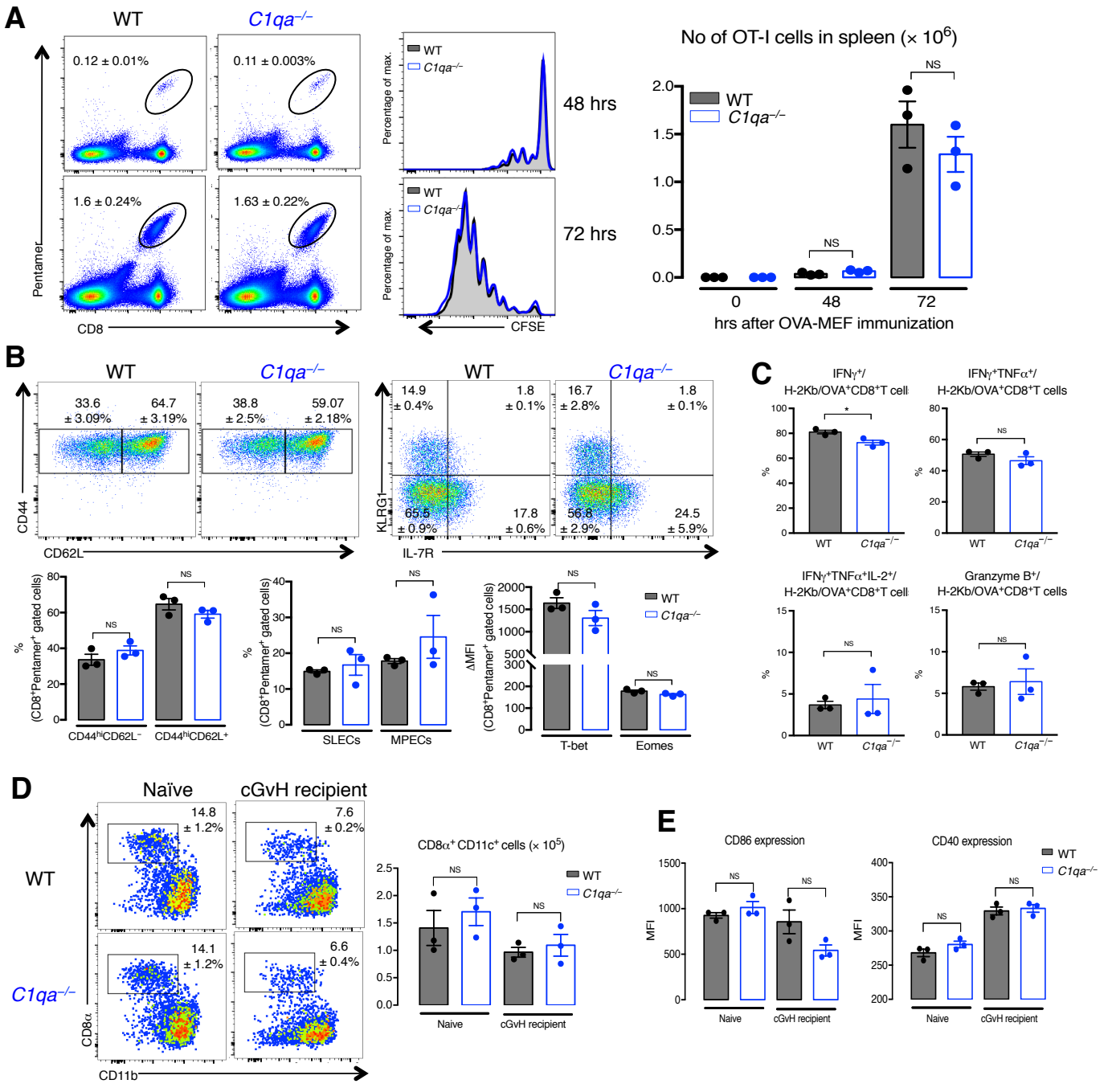

Fig. S4. Cross-priming of apoptotic cell-associated antigens by CD8α$^+$ DCs is unaffected by C1q deficiency. **(A** to **C)** OT-I cells were transferred into WT or *C1qa*$^{-/-}$ mice, followed a day later by immunization with UV-treated OVA-MEFs. **(A)** Spleen OT-I proliferation at 48 and 72 hrs after immunization. Representative flow plots of CFSE dilution (gated CD8$^+$pentamer$^+$ cells) and number of splenic OT-I cells (right panel). **(B)** OT-I phenotype at day 5 after immunization. Representative flow plots and percentages of OT-I positive for CD44, CD62L, KLRG1, IL-7R, T-bet and Eomes (gated CD8$^+$pentamer$^+$ cells) are shown. **(C)** Percentages of splenic OT-I cells at day 5 producing IFN-γ, TNF-α, IL-2 and Granzyme B following 4 hrs incubation with OVA peptide. **(D)** Representative flow plots (left, gated CD11c$^+$ cells) and number (right) of CD8α$^+$ DCs in WT and *C1qa*$^{-/-}$ mice 7 days after cGvH induction. Spleens from naïve mice were used as controls. **(E)** Expression of CD86 and CD40 on CD8α$^+$ DCs described in **D**. NS: non significant; *$p<0.05$; unpaired Student's *t*-test. Data are mean ± SEM and represent two (**B,C**) or three experiments (**A,D,E**) (n = 3 mice/group).

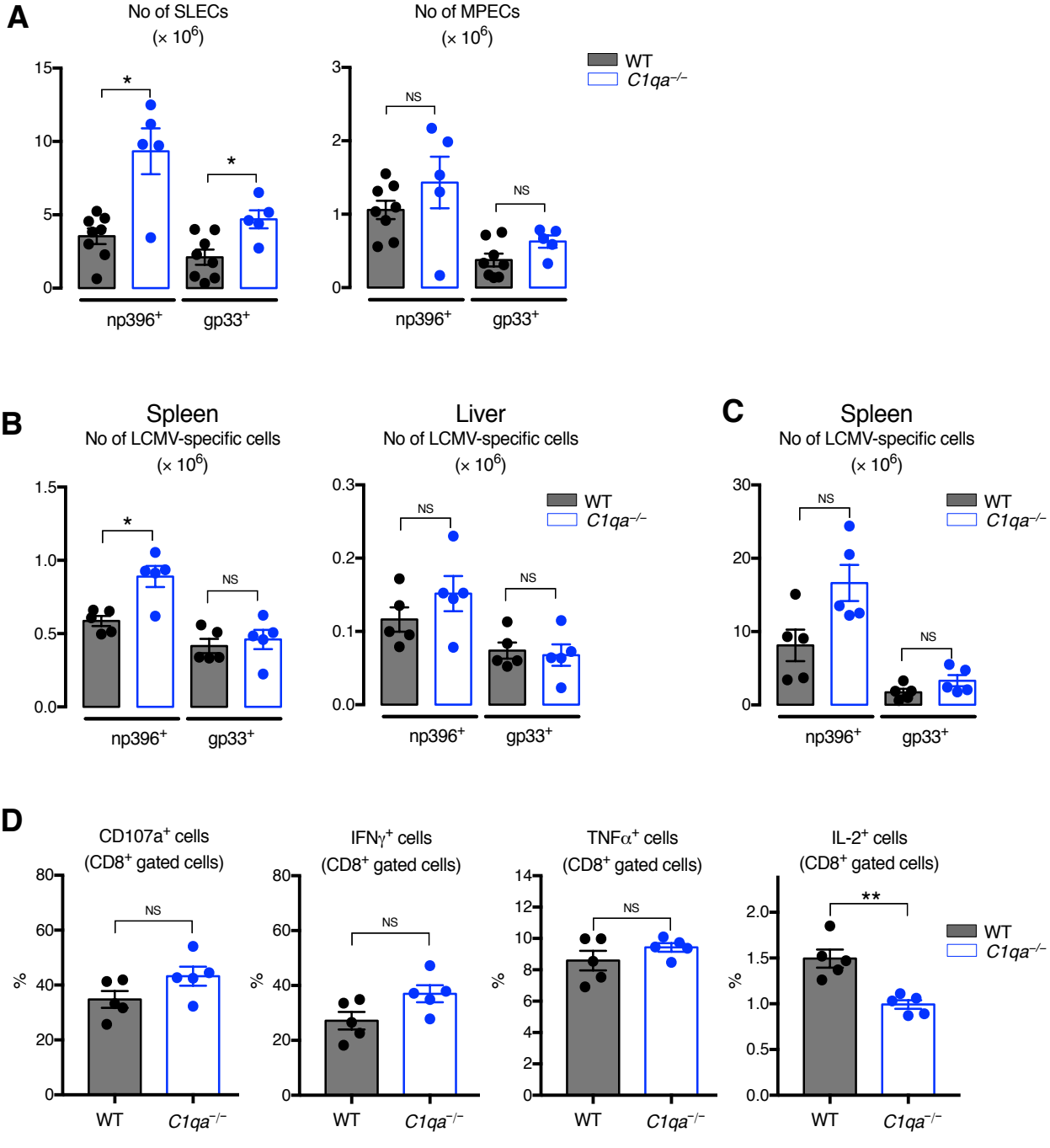

Fig. S5. LCMV-specific memory CD8⁺ T-cell responses in WT and *C1qa*$^{-/-}$ mice. (A to **B)** WT and *C1qa*$^{-/-}$ mice were infected with LCMV-Arm. **(A)** Numbers of splenic np396⁺ and gp33⁺ SLECs and MPECs at day 8. **(B)** Numbers of np396⁺ and gp33⁺ CD8⁺ T cells in spleen (central memory) and liver (effector memory) at day 30 after infection. **(C** to **D)** WT and *C1qa*$^{-/-}$ mice were infected with LCMV-Arm. Sixty days later, mice were re-challenged with LCMV-Cl13. LCMV-specific CD8⁺ T cells were examined at day 7 after re-infection. **(C)** Numbers of np396⁺ and gp33⁺ CD8⁺ T cells in spleen. **(D)** Percentage of splenic CD8⁺ T cells expressing CD107a and proportions of IFN-γ, TNF-α and IL-2-producing CD8⁺ T cells after in vitro re-stimulation with LCMV peptides. NS: non significant; **p*<0.05, ***p*<0.01; unpaired Student's *t*-test. Data are mean ± SEM; (n = 5 mice/group).

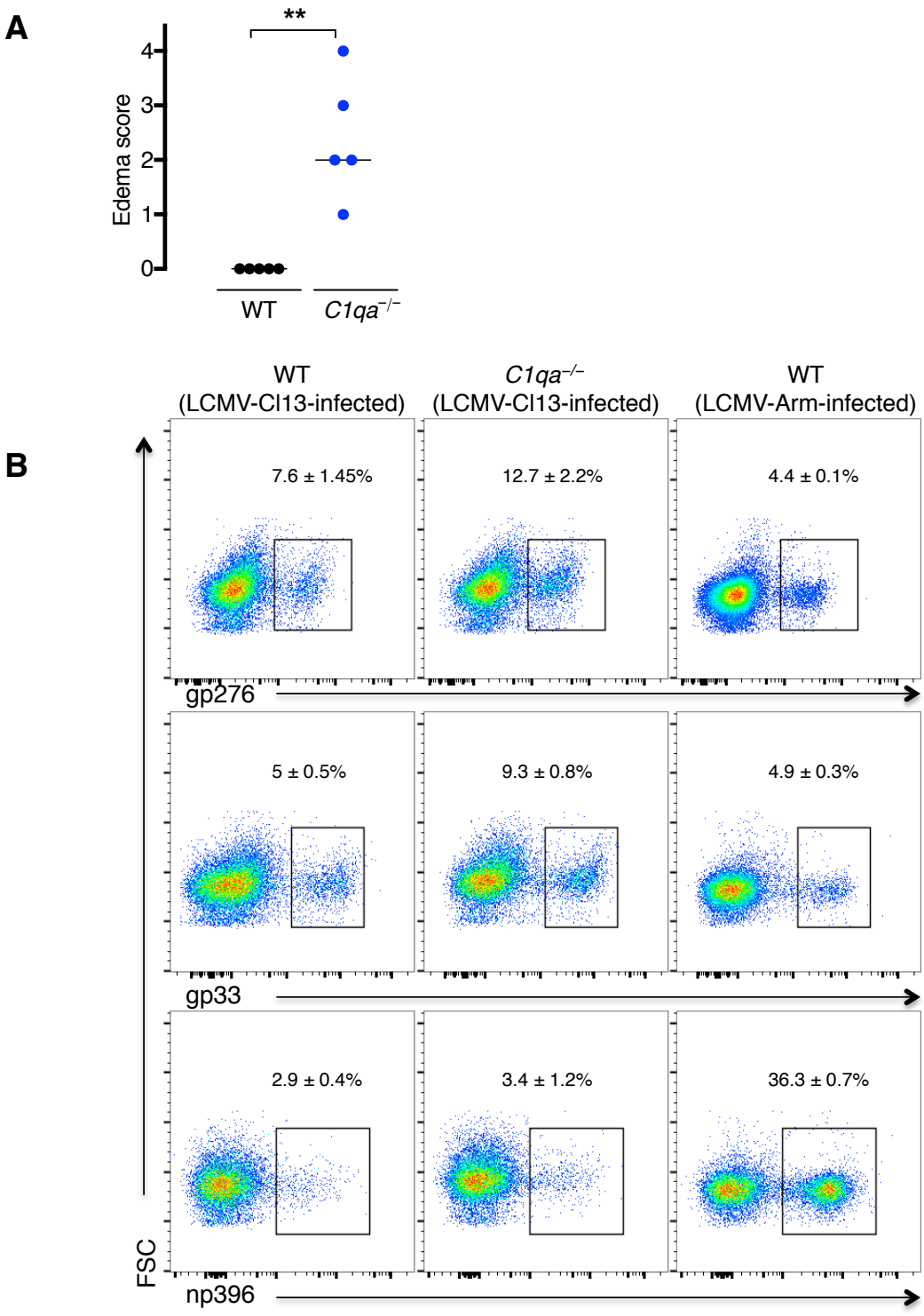

Fig. S6. **LCMV-specific CD8$^+$ T cells and lung edema score in WT and *C1qa*$^{-/-}$ mice after LCMV-Cl13 infection. (A)** Edema score of lung sections at day 11 after LCMV-Cl13 infection. Bars indicate the median. $^{**}p<0.01$; Mann–Whitney test. Data represent two experiments (n = 5 mice/group). **(B)** Representative flow plots of LCMV-specific dextramer staining among splenic CD8$^+$ T cells at day 11 after LCMV-Cl13 infection. LCMV-Arm-infected WT mice were used as control to set gating regions. Percentages of positive cells are shown. Data are mean ± SEM(n = 3-5 mice/group).

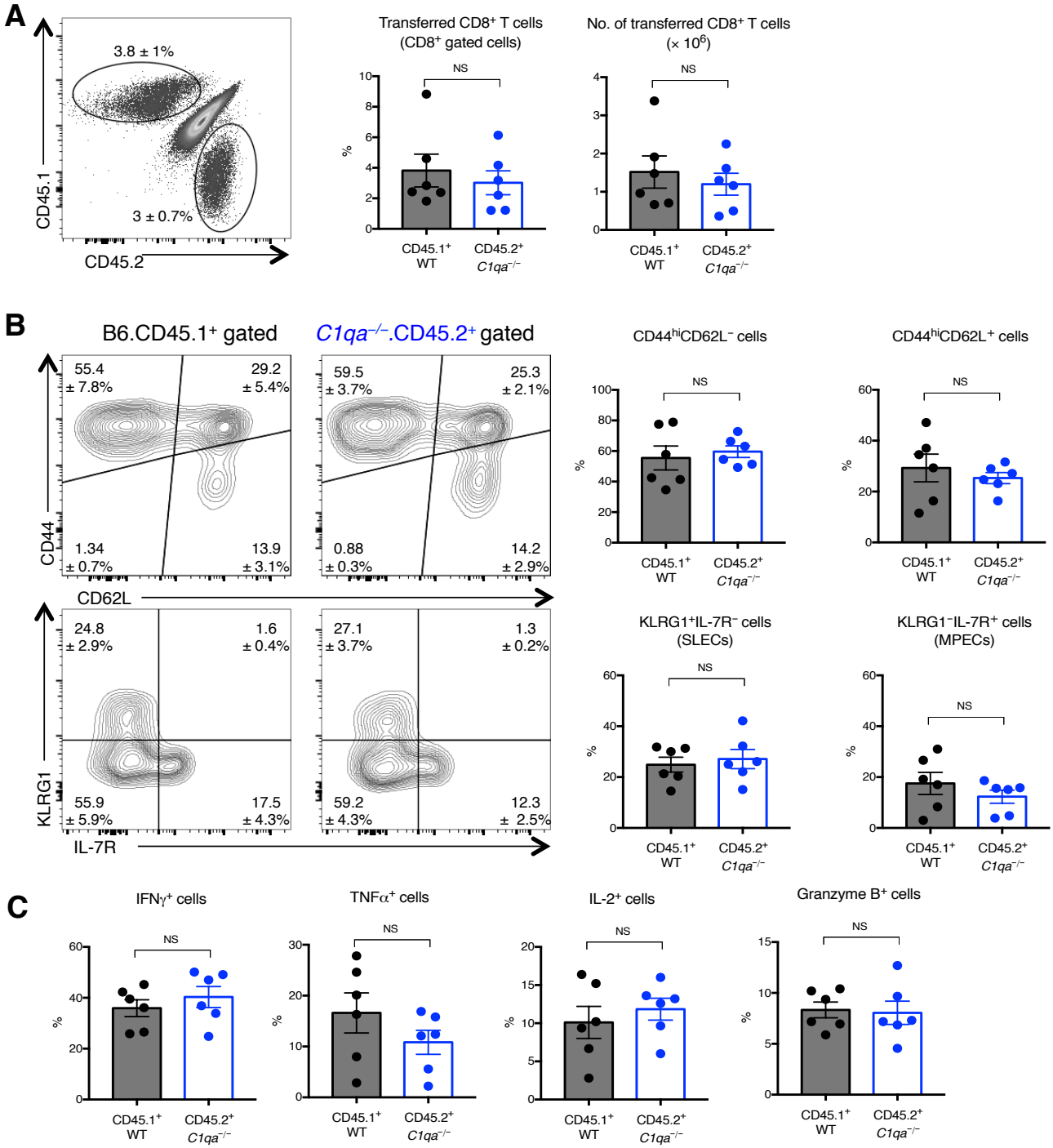

Fig. S7. C1q affects CD8⁺ T cells via an extracellular pathway. Isolated naïve CD8⁺ T cells from B6.CD45.1⁺ and *C1qa*$^{-/-}$.CD45.2⁺ mice were co-transferred (1:1 ratio) into B6.CD45.1⁺.CD45.2⁺ mice. One day later the recipients were i.p. injected with bm12 CD4⁺ T cells. Adoptively transferred cells were analyzed 14 days after GvH induction. **(A)** Representative flow plot of CD45.1 and CD45.2 staining in GvH-recipient spleens (gated CD8⁺ T cells). Frequency and number of adoptively transferred cells recovered from the spleens are shown. **(B)** Representative flow plots of CD44, CD62L, KLRG1 and IL-7R expression in the transferred cells. Frequencies of each CD8⁺ T-cell subset are presented. **(C)** Percentages of adoptively transferred B6.CD45.1⁺ and *C1qa*$^{-/-}$.CD45.2⁺CD8⁺ T cells producing IFN-γ, TNF-α, IL-2 and Granzyme B after in vitro re-stimulation with PMA/Ionomycin. NS: non significant; unpaired Student's *t*-test. Data are mean ± SEM and represent two experiments (n = 6 mice/group).

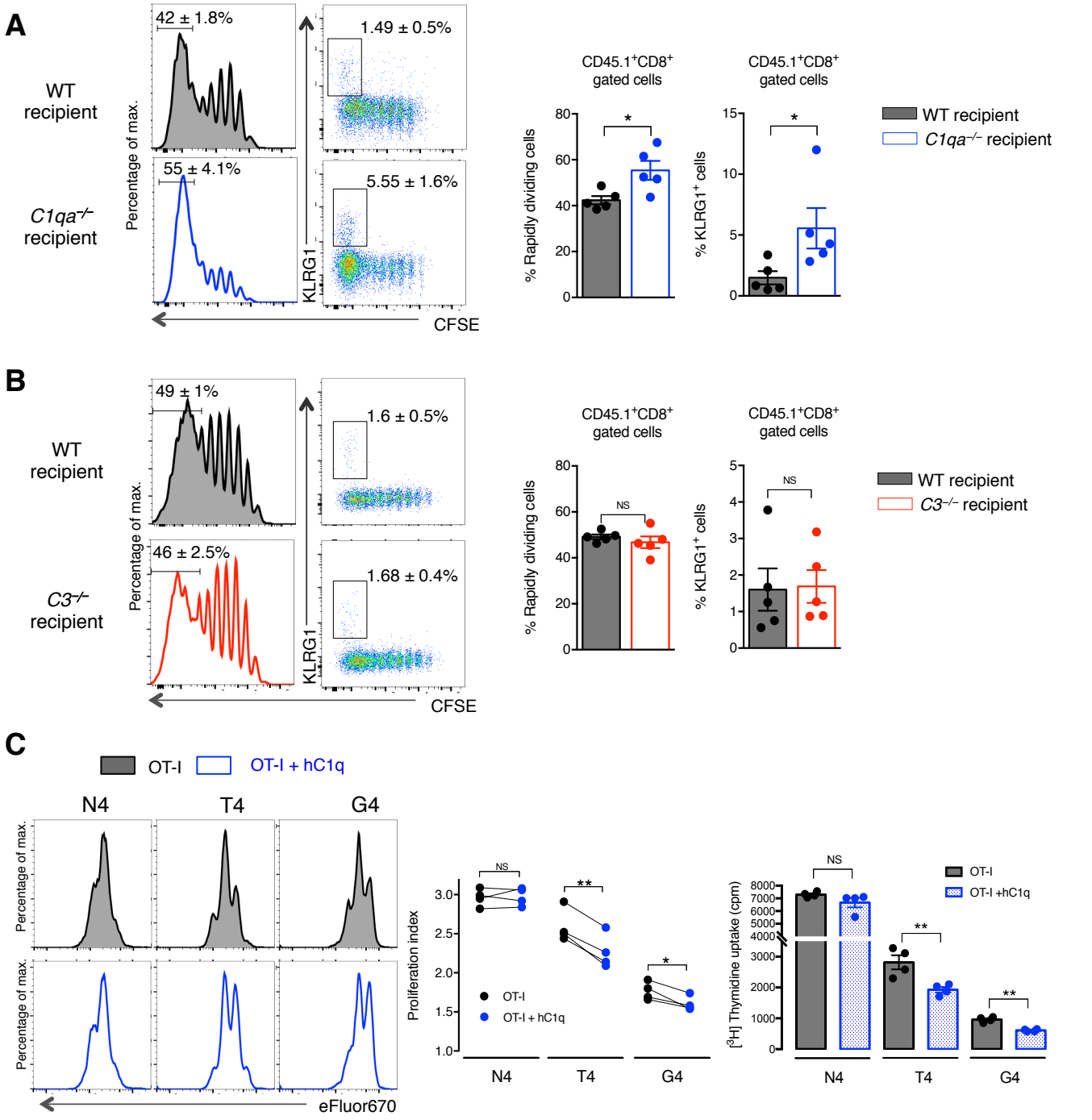

Fig. S8. C1q restrains CD8$^+$ T-cell activation and proliferation triggered by weak agonists. (A to **B)** Naïve CFSE-labelled B6.CD45.1$^+$CD8$^+$ T cells were adoptively transferred into antibiotic-treated sub-lethally irradiated B6.CD45.2$^+$ and *C1qa*$^{-/-}$ hosts (n = 5 mice/group) (**A**) or B6.CD45.2$^+$ and *C3*$^{-/-}$ hosts (n = 5 mice/group) (**B**). Donor cell proliferation and activation were analyzed 14 days later. Representative flow plots and frequencies of fast-proliferating and activated donor B6.CD45.1$^+$CD8$^+$ T cells in the spleen. (**C**) eFluor670-labelled OT-I cells (four biological replicates) were stimulated, in the presence or absence of 80 µg/ml of hC1q, with three OVA-peptides (10^{-6} M): agonist SIINFEKL (N4), partial agonist SIITFEKL (T4), or very weak agonist SIIGFEKL (G4). Cell proliferation assessed by eFluor670 dilution or thymidine incorporation. NS: not significant; *p<0.05; **p<0.01; unpaired Student's t-test **(A** and **B)** or paired Student's t-test **(C)**. Data are mean ± SEM and represent three experiments.

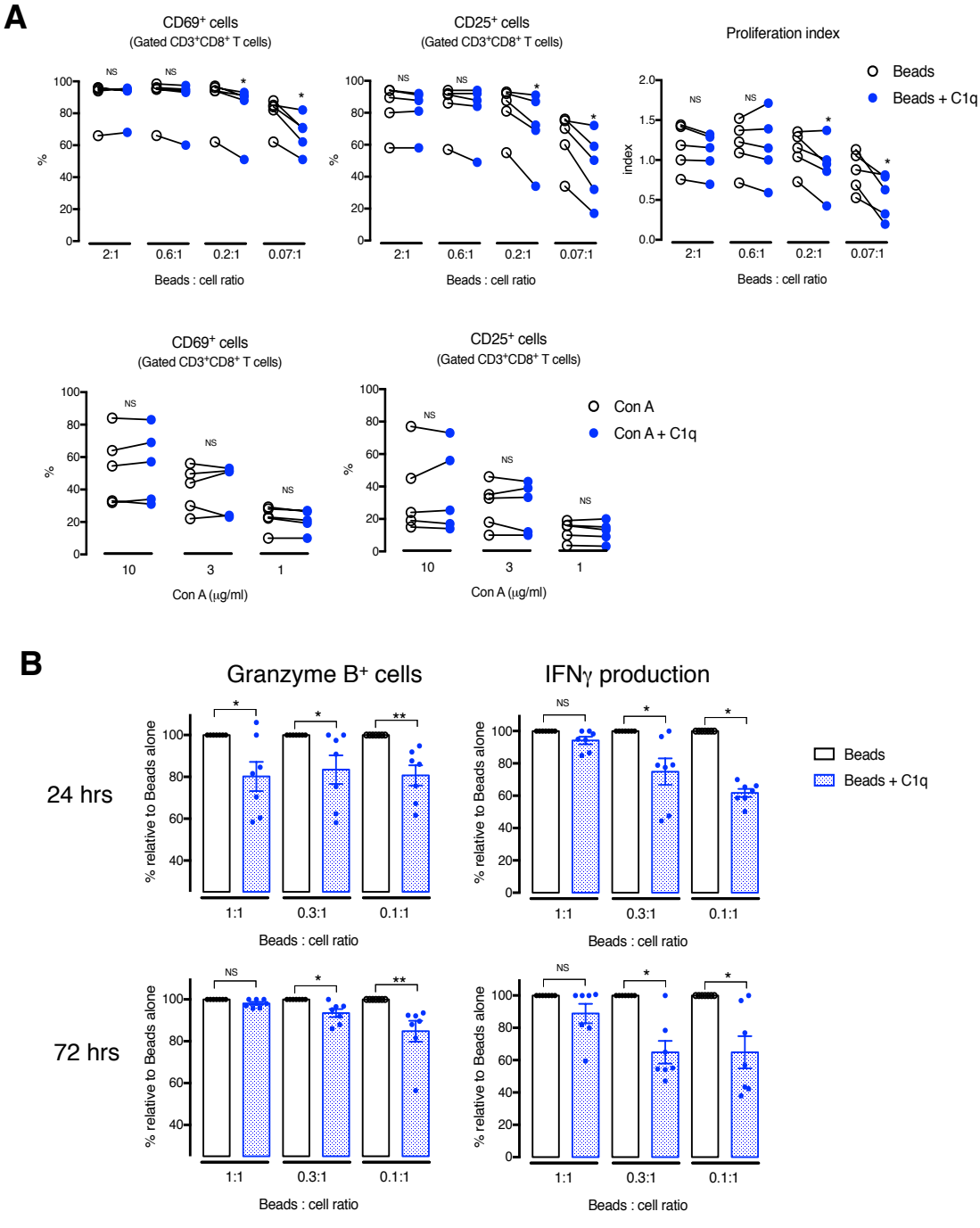

Fig. S9. C1q inhibits human CD8$^+$ T-cell activation, proliferation and cytotoxic function under suboptimal anti-CD3/CD28 stimulation. (A) Peripheral blood mononuclear cells (PBMCs) from five healthy donors were labelled with CFSE and stimulated (10^5/well) with different doses of anti-CD3/CD28 beads or ConA in the presence or absence of 50 μg/ml hC1q. CD69 and CD25 expression on CD3$^+$CD8$^+$ T cells were assessed at 24 hrs. The proliferation index of CD3$^+$CD8$^+$ T cells was assessed at 72 hrs. **(B)** Isolated human CD8$^+$ T cells were stimulated with anti-CD3/CD28 beads at different ratios in the presence or absence of 50 μg/ml hC1q. Granzyme B-expressing cells and IFN-γ production were assessed at 24 and 72 hrs. The data were normalized to the corresponding values without C1q. NS: non significant; *p<0.05; **p<0.01; paired Student's t-test **(A)** or Wilcoxon signed–rank test **(B)**. Each symbol represents an individual donor.

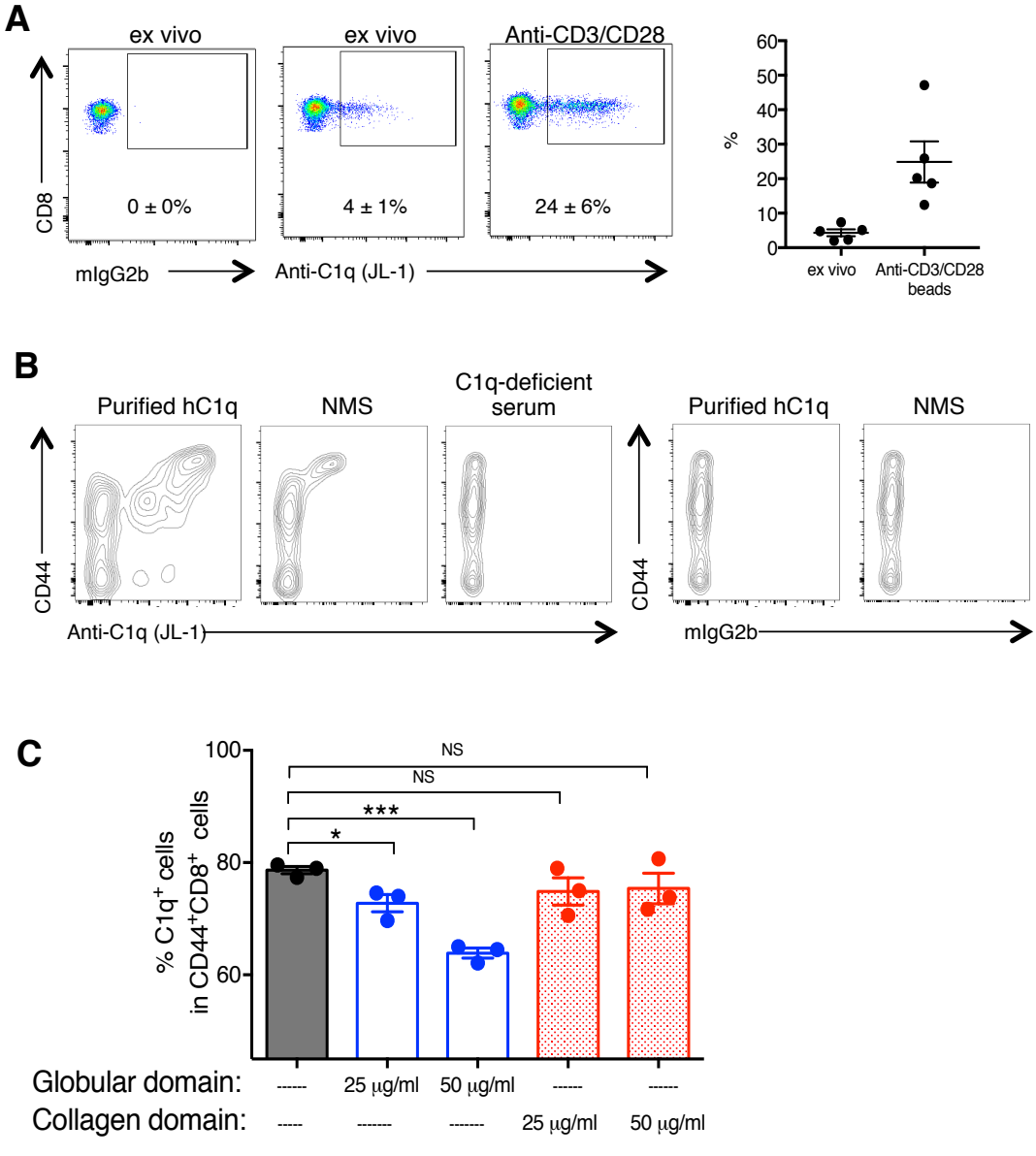

Fig. S10. Inhibition of C1q binding on CD8⁺ T cells by the globular domain. (A) Blood samples from healthy donors were left untreated (ex vivo) or activated with anti-CD3/CD28 beads for 1 hr. Representative plots of C1q staining (clone JL-1) on gated $CD3^+CD8^+$ T cells and percentage of $CD3^+CD8^+$ T cells positive for C1q (right panel). Each symbol represents an individual donor. **(B)** Blood from *C1qa*$^{-/-}$ mice was incubated with 80 μg/ml hC1q or 30% normal mouse serum (NMS) or C1q-deficient serum and stained with anti-C1q antibody or an isotype control. Representative flow plots (gated $CD8^+$ T cells). **(C)** Blood from *C1qa*$^{-/-}$ mice was incubated with the globular or collagen domain prior to adding hC1q (two doses). Percentage of $CD44^+CD8^+$ T cells positive for C1q was quantified by flow cytometry. NS: not significant; *p<0.05; ***p<0.001; unpaired Student's t-test. Data are mean ± SEM and represent three experiments (n = 3) **(C)**.

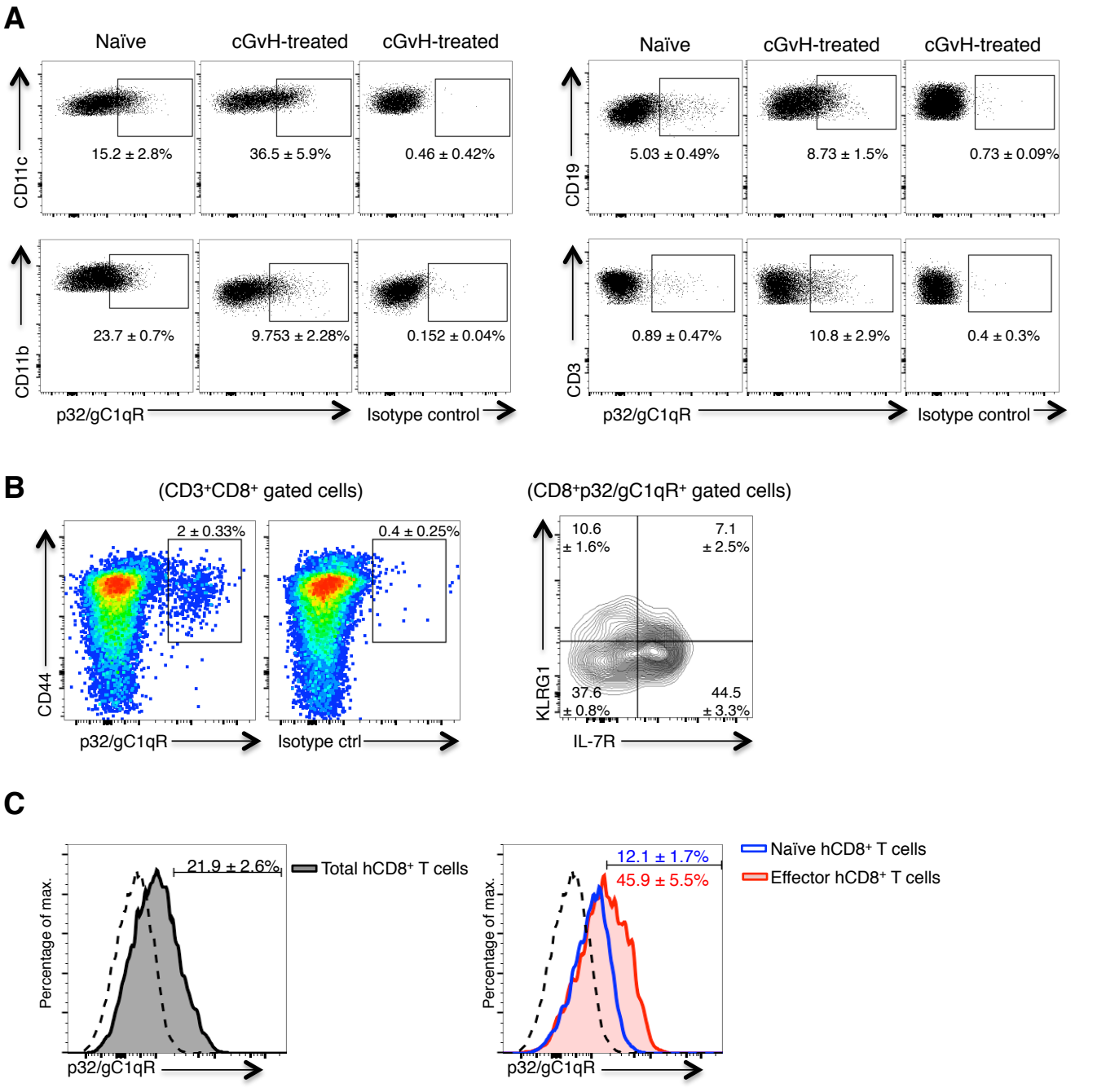

Fig. S11. Surface expression of p32/gC1qR on immune cells and activated CD8$^+$ T cells. (A) Representative flow plots of p32/gC1qR expression among WT splenic CD11c$^+$ DCs, CD11b$^+$ macrophages, CD19$^+$ B cells and CD3$^+$ T cells two weeks after bm12-cGvH induction. Cells from naïve mice are shown as controls. Percentages of positive cells are indicated. **(B)** Representative flow plots of CD44 and p32/gC1qR expression within WT splenic CD8$^+$ T cells two weeks after cGvH induction (left and middle panel). KLRG1 and IL-7R expression within CD8$^+$p32/gC1qR$^+$ T cells (right panel). Percentages of positive cells are indicated. **(C)** p32/gC1qR expression on human PBMCs. Representative histograms from four donors of CD3$^+$CD8$^+$ T cells (left panel), naïve (CCR7$^+$CD45RA$^+$) and effector (CCR7$^-$CD45RA$^+$) CD8$^+$ T-cell subsets (right panel). Dotted lines indicate isotype control. Percentages of positive cells are shown. Data are mean ± SEM and represent two experiments (n = 2-4/experiment) **(A** and **B)**.

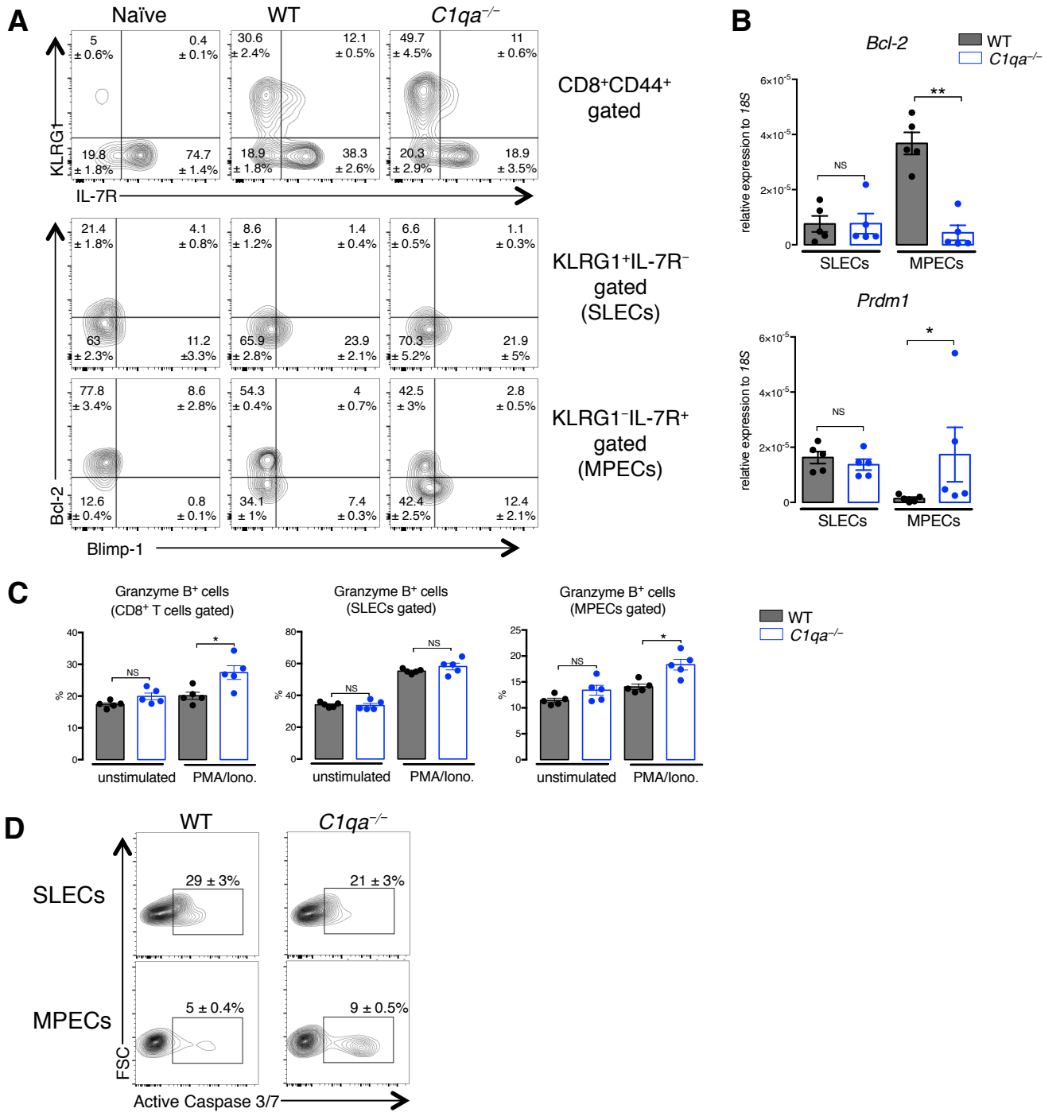

Fig. S12. Abnormal profile of C1q-deficient MPECs. (A) Representative plots of KLRG1 and IL-7R expression (gated $CD8^+CD44^+$ T cells) and intracellular staining of Bcl2 and Blimp-1 within SLEC and MPEC gated subsets from naïve or bm12-cGvH-recipients (WT or *C1qa*$^{-/-}$) two weeks after induction. Percentage of positive cells indicated. **(B)** *Bcl-2* and *Prdm1* mRNA expression in sorted splenic SLECs and MPECs two weeks after cGvH induction. **(C)** Fractions of SLECs and MPECs positive for Granzyme B two weeks after cGvH induction. **(D)** Representative plots of active Caspase 3/7 expression within SLECs and MPECs three weeks after cGvH induction NS: not significant; *p<0.05; **p<0.01; unpaired Student's t-test. Data are mean ± SEM and are representative of three experiments (n = 3-5 mice/group).

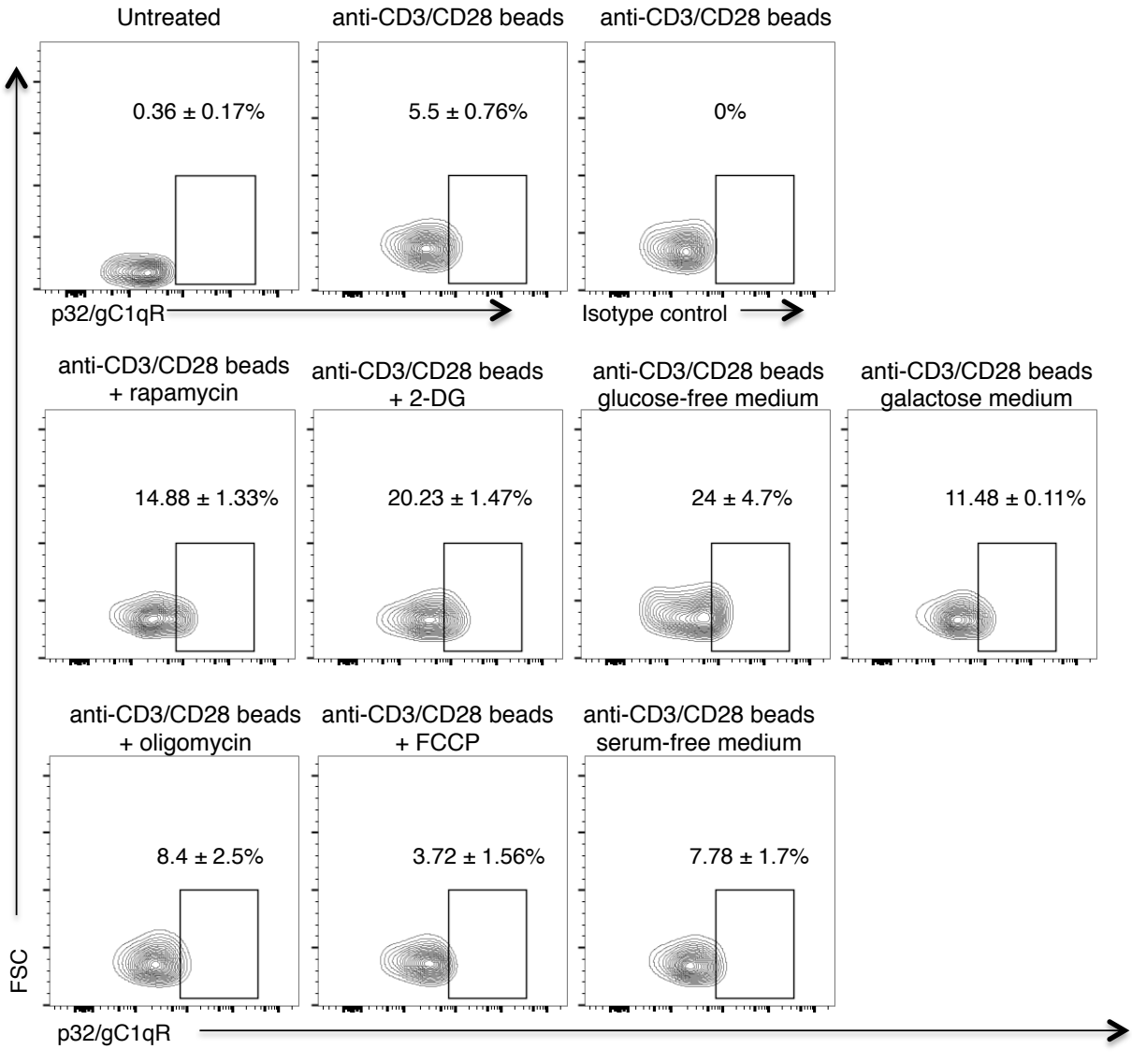

Fig. S13. Glucose deprivation increases the surface expression of p32/gC1qR on activated CD8$^+$ T cells. Mouse naive CD8$^+$ T cells were left untreated or activated with anti-CD3/CD28 beads in the presence of: i) rapamycin, a mTORC1 inhibitor that reduces glycolysis, (500 nM); or ii) 2-deoxyglucose (2DG) (50 mM); or iii) glucose-free medium; or iv) galactose medium (10 mM) (to prevent cells utilizing glycolysis); or v) oligomycin (10 nM); or vi) fluorocarbonylcyanide phenylhydrazone (FCCP) (10 nM); or vii) serum-free medium. p32/gC1qR surface expression was measured by flow cytometry. Representative flow plots are shown. Data are mean ± SEM and representative of three experiments (n = 4 mice/group).

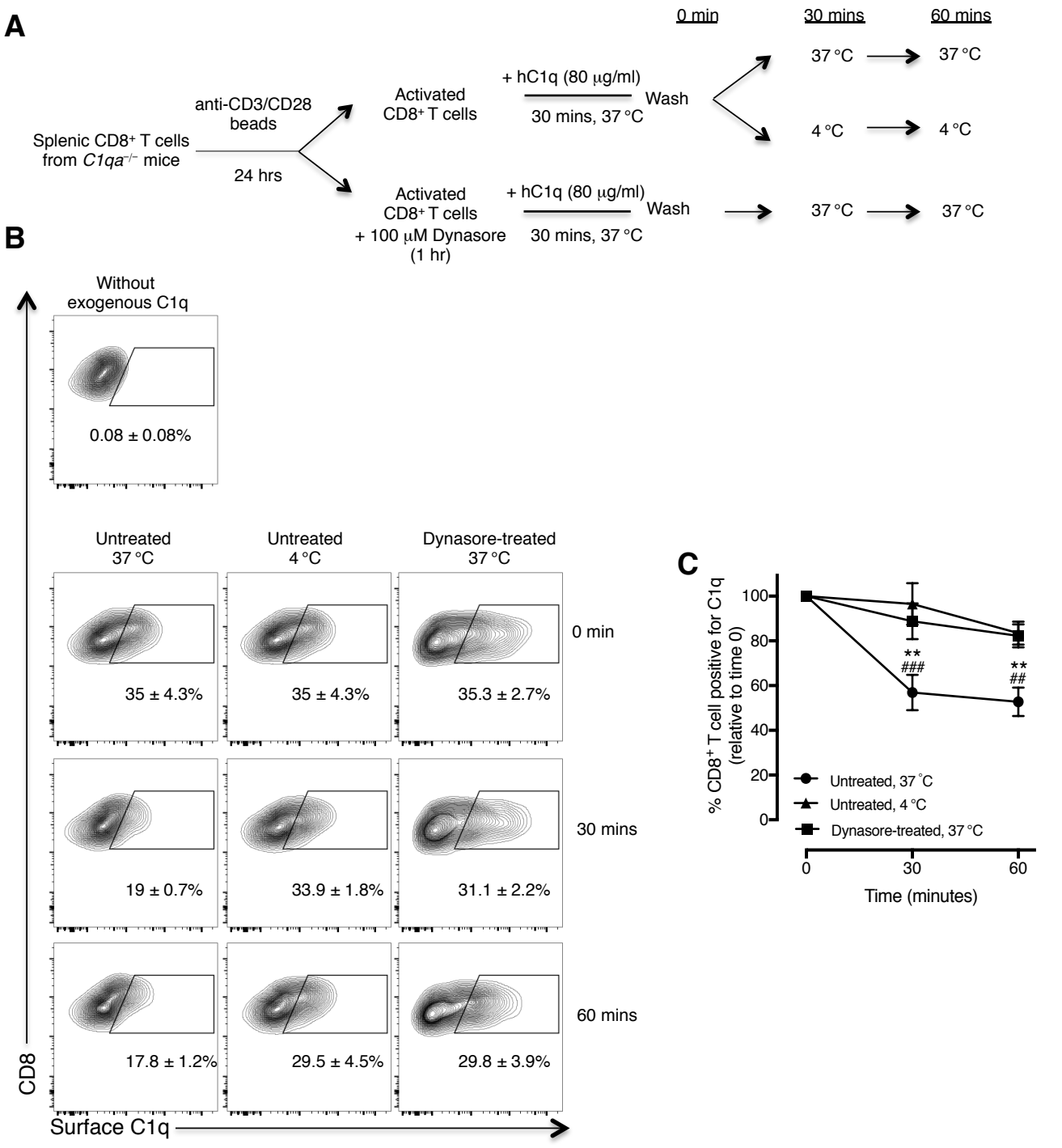

Fig. S14. Internalization of surface-bound C1q on activated CD8⁺ T cells. (A) Schematic outline of the experimental protocol. The surface expression of C1q on activated splenic CD8⁺ T cells was assessed by flow cytometry with an anti-C1q antibody (clone JL-1) at three time points: 0, 30, and 60 minutes. **(B)** Representative flow plots of surface C1q staining. Percentages of positive cells are shown. **(C)** Kinetics of surface loss of C1q under the different conditions at the indicated times. Displayed are the percentages of C1q positive cells at each time point relative to the corresponding time 0. Two-way ANOVA; $^{**}p<0.01$ (untreated vs Dynasore-treated cells at 37 °C); $^{\#\#}p<0.01$, $^{\#\#\#}p<0.005$ (untreated at 37 °C vs untreated at 4 °C) . Data are mean ± SEM and representative of two experiments (n = 4 mice/group).

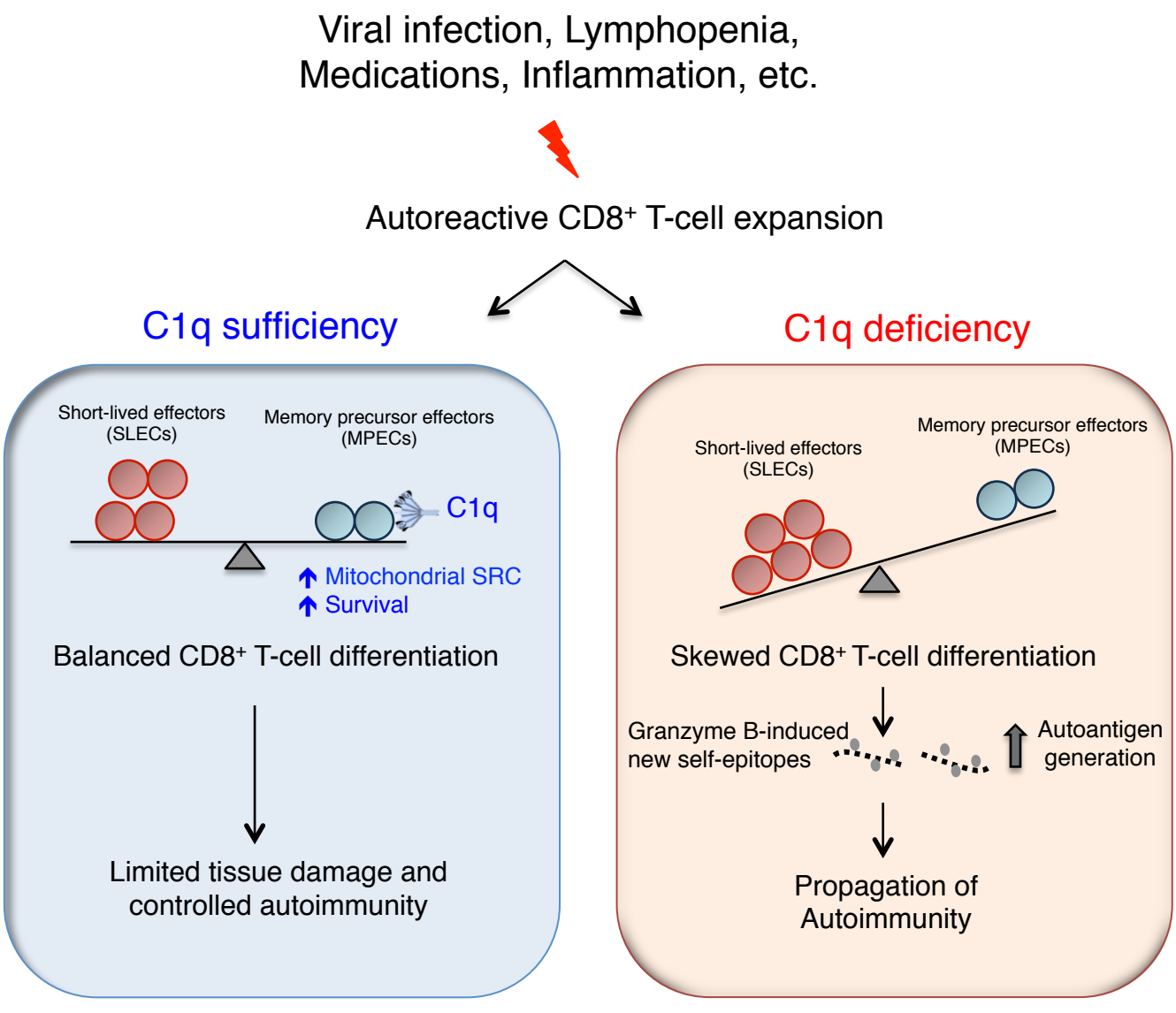

Fig. S15. Schematic illustration of the proposed role of C1q in CD8$^+$T-cell responses. Several triggers, including viruses and lymphopenia, can induce CD8$^+$T-cell expansion and differentiation. C1q, independently of complement activation, promotes balanced effector CD8$^+$ T-cell responses by acting as a metabolic regulator and increasing the mitochondrial spare respiratory capacity (SRC). This C1q-mediated effect restrains the propagation of autoimmunity and limits immunopathology in chronic viral infections. This new role of C1q may explain how this molecule prevents lupus flares during a viral infection.